Physica B: Condensed Matter 570 (2019) 274–279

Contents lists available at ScienceDirect

Physica B: Condensed Matter

journal homepage: www.elsevier.com/locate/physb

Impact of iron atoms on electronic properties of FZ n-Si with dislocations☆

Maria Khorosheva, Vitaly Kveder*, Alexey Tereshchenko

Institute of Solid State Physics, Russian Academy of Sciences, 142432, Chernogolovka, Russia

ARTICLE INFO

Keywords:
Silicon
Dislocations
Iron
DLTS
LBIC
Defects

ABSTRACT

Impact of iron atoms on electronic properties of FZ n-Si containing dislocations introduced by plastic deformation is studied using deep level transient spectroscopy (DLTS) and laser beam induced current (LBIC). Amplitudes of dislocation related DLTS peaks "C1" at 201 K and "D" at 247 K increase significantly after diffusing iron at 900 °C in the samples quenched after diffusion. DLTS and LBIC data correlate nicely showing a significant increase of electron-hole recombination at dislocations in the same samples. We therefore suppose that the DLTS peaks "C1" and "D" observed earlier in many publications can be partially related to iron at dislocations.

1. Introduction

Multi-crystalline silicon (mc-Si) that is widely used for solar cell manufacturing usually contains relatively high concentration of transition metal impurities and, at the same time, has quite a high concentration of dislocations. In a dissolved state those impurities act as very effective centers of electron-hole recombination which reduces solar cells efficiency of [1–5]. The only way to produce highly efficient inexpensive mc-Si solar cells is to increase average diffusion length of minority carriers by using the "defect engineering" based on deeply studying the properties of the above-mentioned impurities and other defects in Si. In monocrystalline Si the properties and behavior of transition metal atoms have been investigated quite well [6–9]. But dislocations may significantly influence the behavior of transition metal atoms [10–12]. This fact makes investigating the interaction of impurities with dislocations, as well as electronic properties of dislocations contaminated by these impurities, greatly interesting.

Iron is one of the dangerous impurities often found in solar grade silicon. It is well known that interstitial iron atoms Fe_i and Fe_iB_s pairs in p-Si may significantly reduce the minority carrier lifetime [6,13,14]. Interstitial iron atoms Fe_i have one deep donor level in a silicon band gap at $E_{Fei} = E_V + 0.4$ eV [15–18]. Since the diffusion coefficient remains high even at room temperature, the positively charged iron atoms in p-Si can react with negatively charged boron atoms forming the iron-boron pairs which have a donor level at $E_{FeB\text{-}d} = E_V + 0.1$ eV and an acceptor level at $E_{FeB\text{-}a} = E_C - 0.26$ eV [19,20]. Here E_C and E_V correspond to the energy of the conduction band bottom and the valence band top of crystalline Si respectively.

There isn't much information about the behavior of iron atoms in silicon in presence of dislocations, as well as how iron influences the electronic properties of dislocations. Here we investigate the influence of iron on electronic properties of FZ-n-Si samples containing dislocations. We controlled the electrical properties of the samples before and after iron in-diffusion by using deep level transient spectroscopy (DLTS) and light beam induced current (LBIC).

Theoretical calculations [12] predict that segregation of Fe atoms at Shockley dislocations should be energetically favorable. The electronic properties of iron atoms in dislocation core must differ significantly from the properties of interstitial iron atoms in the bulk of silicon. The electronic energy level of Fe atoms located in dislocation core should be by 0.42 eV higher than that of Fe_i level in Si bulk. So it should be at about *Ec* - 0.35 eV [12].

In n-Si samples, the effect of iron atoms on the electronic properties of silicon was studied mainly in dislocation-free samples [26–29]. After iron diffusion, 3 or 4 new peaks were detected in the DLTS spectra in n-Si samples [26–28]. With the exception of a defect with E_C - 0.35 eV, the defects responsible for these peaks are not thermally stable and disappear when the sample is held at room temperature or during annealing at 200 °C. It was supposed that the deep level at E_C - 0.35 eV is associated with Fe_s [27]. Indeed, according to theoretical calculations [24,25], the reaction of interstitial iron with a single Si vacancy $Fe_i + V \rightarrow Fe_s + 2.6$ eV should be energetically favorable. In addition to

☆ Impact of iron atoms on the electronic properties of Si containing dislocations is investigated by the DLTS and LBIC. In samples quenched after iron diffusion, the e-h recombination rate at dislocations increases significantly in correlation with increasing of DLTS peaks at 201 K and at 247 K. We therefore suppose that these DLTS peaks are associated with iron at the dislocations.

* Corresponding author.
E-mail address: kveder@issp.ac.ru (V. Kveder).

https://doi.org/10.1016/j.physb.2019.06.007
Received 26 March 2019; Received in revised form 2 June 2019; Accepted 4 June 2019
Available online 07 June 2019
0921-4526/

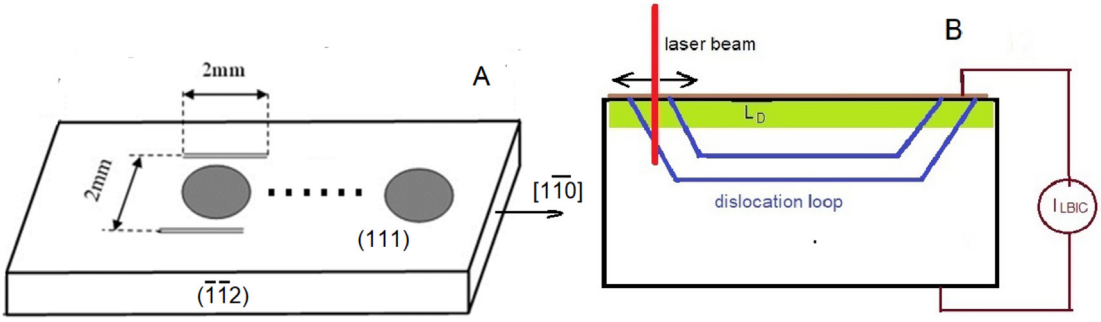

Fig. 1. A sketch illustrating the sample geometry and orientation (A), and LBIC geometry (B). A main contribution to LBIC current comes from the holes generated in the area which is about as thick as the diffusion length $L_D = (D\,\tau)^{1/2}$. The size of dislocation half-loops is usually larger than L_D. So, only some parts of dislocation loops at the depth from 0 to L_D can be visible in LBIC images.

substitutional iron atoms Fe_s, it can result in metastable {Fe_iV} complex. However, theoretical calculations predict that Fe_s should be electrically inactive. The {Fe_iV} should be electrically active, but its energy level should be at about E_V + 0.35 eV. So it cannot be observed by DLTS in n-Si. At the same time, the deep level parameters at E_C - 0.35 eV observed in Ref. [27] are very close to the FeAu complex [30].

In this paper, we present the results of DLTS and LBIC studies of FZ-n-Si samples containing dislocations before and after Fe in-diffusion.

2. Materials and methods

Samples 32 x 4 x 1.3 mm^3 in size were cut from floating zone silicon (FZ-Si) single-crystal of n-type with phosphorus concentration of about 10^{14} cm^{-3}. The face orientations of the samples were (110), (112) and (111).

Dislocations were produced by a plastic deformation of samples using four-point bending at a temperature of 600°C with a load of 30 MPa. Diamond indenter pits at the (111) plane in the sample region for LBIC measurements, and two parallel scratches 2 mm long in the region for DLTS measurements acted as the sources of dislocations (see Fig. 1A). The dislocation density N_D was determined by counting the etching pits. In the DLTS measurement regions (between scratches) it usually was about N_D = (1–2) x 10^5 cm^{-2}.

After deformation, all samples were mechanically polished to remove a layer of about 20 μm, and then chemically polished in HF:7HNO_3. All samples were subjected to aluminum gettering (AlG) before iron diffusion. For AlG, a layer of pure Al of about 1 μm thick was deposited on (111) surface of a sample. Then the sample was kept in argon atmosphere at a temperature of 830 °C for 2 h and slowly cooled to 400 °C. Sample preparation was similar to the one described in Refs. [11,21].

Iron diffusion was carried out from an iron layer (3 N), which was thermally evaporated in vacuum on (111) surface of samples. Samples were placed in an argon flow in a quartz tube and kept at a temperature 900 °C for 1 h. Some of the samples were cooled slowly in the same quartz tube when taken out of the furnace, but some of the samples were quenched in ethylene glycol or 10% NaOH water solution. After diffusion, a layer of about 30 μm was removed from the sample surface by mechanical and chemical polishing. The [Fe_i] iron atoms solubility can be calculated by an equation $[Fe_i] = 5 \times 10^{22} \exp(7.3–2.87\ eV/kT)$ cm^{-3} [15]. After in-diffusion at 900 °C, a total iron concentration should be about 4×10^{13} cm^{-3} at a depth of 20–30 μm.

To measure the DLTS spectra two gold Schottky contacts 2 mm in diameter were evaporated in vacuum at the (111) sample surface: one to the sample area with about 10^5 cm^{-2} dislocations, and another to the dislocation-free area (the control area) of every sample (see Fig. 1A). For LBIC measurements, a semitransparent gold Schottky contact was deposited on the whole (111) surface of the sample. An Ohmic contact was a layer of AlGa eutectic on the back side of the sample.

The maps of diffusion length $L_D = (D\,\tau)^{1/2}$ of the minority carriers (holes) were calculated from the LBIC maps of electric current induced in a Schottky contact by laser beam scanning of the (111) surface of the sample (see Fig. 1B). The laser beam diameter was about 5 μm. The laser wavelength was 980 nm. For light with this wavelength the absorption coefficient in Si is about $\alpha = 67\ cm^{-1}$. The average value of L_D under the laser spot was calculated using the well-known expression for the LBIC current I_{LBIC}, generated by a photo-excited holes diffusion from a sample to a Schottky contact on its surface: $I_{LBIC} = I_0/(1 + 1/\alpha L_D)$ [31]. Here the I_0 is a maximal current that only depends on the photon flux penetrating into the sample.

The dislocation half-loops in our samples were usually of larger size than the diffusion length $L_D = (D\,\tau)^{1/2}$ of holes. So, only parts of dislocation loops at a depth of about L_D or smaller under the Schottky contact can be visible in LBIC map images (see Fig. 1B).

3. Results and discussion

Fig. 2 shows the maps of the minority carrier diffusion lengths L_D in the areas with large dislocation loops, measured before and after iron diffusion in n-Si samples. The L_D maps were calculated from the maps of LBIC current. Fig. 2a show the L_D map before iron in-diffusion, while Fig. 2b, c and d show the L_D-maps after in-diffusion of Fe at 900 °C in samples cooled with different rates after diffusion.

It can be seen that before Fe in-diffusion (Fig. 2a), the diffusion length L_D was quite uniform and exceeded 150 μm. It follows from the L_D-map in Fig. 2a, that neither dislocations nor the “trail”-defects generated during dislocation motion in their slip planes [21–23] give any significant contribution to electron-hole recombination.

Fig. 2b shows L_D map in the sample slowly cooled after iron diffusion. Now the dislocations become visible in the L_D map. It means that e-h recombination rate increased at dislocations, but not very much. The main effect of iron observed in the slowly cooled sample is a significant increase of electron-hole recombination rate τ^{-1} in a vicinity of dislocation slip planes, where we can expect an existence of dislocation “trail”-defects. One can see that L_D in the regions of dislocation slip planes is about 90–100 μm, while in the non-deformed region of the same sample L_D is about 120–140 μm.

We noticed that a similar effect was observed earlier after the diffusion of gold in similar samples [23].

We found earlier that the “trail”-defects were in fact some vacancy complexes Vx_{trail} generated during the dislocation motion [21]. Most of these “trail”-defects are electrically inactive, but can be detected by their reaction with some interstitial metal atoms: $M_i + Vx_{trail} => M_s + (x)$ if substitution atoms M_s are electrically active. We found that this reaction works nicely with gold: $Au_i + Vx_{trail} => Au_s + (x)$, but it does not work with Ni_i [23]. Therefore, the observed increase of recombination in dislocation “trails” region after Fe in-diffusion can be explained assuming the emergence of electrically active complexes {Fe_iV} due to the reaction $Fe_i + Vx_{trail} => \{Fe_iV\} + (x)$.

As one can see in Fig. 2c and d, in the samples quenched after Fe-in-

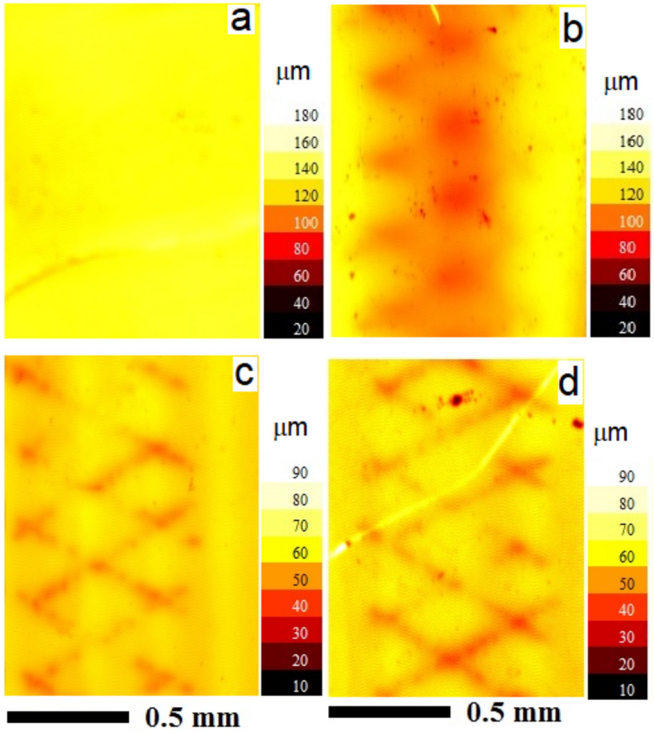

Fig. 2. Maps of holes diffusion length L_D calculated from LBIC, and measured in n-Si samples: (a) - before Fe-in-diffusion; (b) - slowly cooled after Fe-in-diffusion; (c) - quenched in ethylene glycol after Fe-in-diffusion; (d) - quenched in 10% NaOH after Fe-in-diffusion. We can see that the brightness scale for L_D maps (a, b) differs by factor two from the scale for maps (b, c).

diffusion the e-h recombination rate at the dislocations increases very significantly. Now dislocations are much more active in recombination than the regions of "trail"-defects. It can be considered as an indication for a significant increase of deep level defect concentration at dislocations due to their reactions with Fe.

Fig. 3b,c shows the L_D maps in dislocation-free regions of the same samples (b) and (c), as in Fig. 2. Fig. 3b is for slowly cooled sample after Fe-in-diffusion, while sample in Fig. 3c was quenched in ethylene glycol after Fe-in-diffusion. One can see in Fig. 3b,c, that after Fe in-diffusion the L_D decreases also in sample regions that are far away from the regions containing dislocations. However, this decrease is not so dramatic as in the regions with dislocations. Please note that in contrast to the uniform L_D maps in a sample before Fe in-diffusion (see Fig. 2a), the maps in Fig. 3b and c clearly show some "growth ring" (or "striations") contrast.

Such "striations" or "growth rings" can be often observed in any crystals, including Si. They reflect fluctuations of impurities and defect concentrations along the wafer diameter appeared during crystal

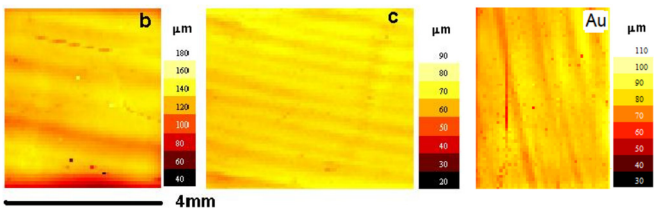

Fig. 3. Maps of hole diffusion length L_D in dislocation-free regions of the same samples (b) and (c) as in Fig. 2 (b, c); (b) the sample slowly cooled after Fe-in-diffusion; (c) - quenched in ethylene glycol after Fe-in-diffusion; Note that the brightness scale for map (b) differs by factor two from the scale for map (c). The L_D map (Au) was measured in dislocation free place of Fz-n-Si sample, but after in-diffusion of gold (3 h at 700 °C) instead of iron.

growth as a result of fluctuations in the microscopic growth rate, temperature gradient and the diffusion boundary layer thickness.

We suppose that the observed striations reflect non-uniform distribution of nitrogen-vacancies complexes usually existing in FZ Si grown in nitrogen ambient [32]. The nitrogen-vacancy complexes (let us call them "VN_x") are electrically inactive in as-grown FZ Si, but can be detected using the reaction $M_i + VN_x = > M_s + N_x$ where M_i is an interstitial metal atom, and M_s is a substitutional metal atom. It was shown that the convenient metal atoms for detection of vacancy-nitrogen complexes are Au, Pt and Ni [33–35]. Fig. 3(Au) shows the L_D-map measured in a dislocation-free place of Fz-n-Si sample, after the in-diffusion of gold (3 h at 700 °C) instead of iron. The non-uniform L_D distribution reflects the non-uniform distribution of electrically active Au_s atoms that appeared due to the reaction $Au_i + VN_x = > Au_s + N_x$. So, the observed "growth rings" correspond to non-uniform distribution of nitrogen-vacancy complexes in as-grown sample. We assume that at least partially the increase of e-h recombination rate in dislocation-free regions after Fe-in-diffusion may come from the generation of electrically active $\{Fe_iV\}$ complexes due to reaction $Fe_i + VN_x = > \{Fe_iV\} + N_x$.

Fig. 4A and Fig. 4B show the DLTS spectra measured in n-Si samples before and after iron diffusion at 900 °C. Fig. 4A shows the DLTS spectra measured in dislocation-free areas before and after Fe-in-diffusion, while Fig. 4B shows the DLTS spectra measured in the areas with dislocation density of about $N_D = 10^5\,cm^{-2}$ in the same samples before and after Fe-in-diffusion. Spectra "a" in Fig. 4A and Fig. 4B were measured before Fe in-diffusion, spectra "b", "c", "d" - after Fe in-diffusion. Spectra "b" corresponds to the sample slowly cooled after Fe in-diffusion, spectra "c" – to the sample quenched to ethylene glycol after Fe in-diffusion and spectra "d" were measured in a sample quenched to 10% NaOH water solution.

The DLTS peak observed in all spectra at 85 K obviously has nothing to do with iron. And it has no correlation with the presence of dislocations. As we see in Fig. 4, the concentration of "85 K" defects, corresponding to the peak at 85 K, vary in different samples from $0.3 \times 10^{11}\,cm^{-3}$ to $3 \times 10^{11}\,cm^{-3}$. We do not know the exact origin of this peak. However, we can suppose that it corresponds to the vacancy-oxygen complexes VO with an energy level at E_C - 0.17 eV [36]. In this paper we are not going to discuss the "85K" defects anymore.

As one can see in Fig. 4A, the concentration of all other defects in dislocation-free regions of all samples is below the noise level ($0.2 \times 10^{11}\,cm^{-3}$), except for the spectrum "d" where one can see a broad DLTS peak at about 230K. However, the amplitude of this peak is also quite small, less or about $0.3 \times 10^{11}\,cm^{-3}$.

We do not see any obvious correlation between the amplitudes of DLTS peaks in Fig. 4A and the average L_D values estimated from LBIC in dislocation-free regions (see Fig. 3b,c and Fig.2A). Please note that if the "striations" in Fig. 3b,c are indeed due to $\{Fe_iV\}$ complexes, the L_D value may not correlate with DLTS data. According to theoretical predictions [24,25], the $\{Fe_iV\}$ complex should have the energy level at about E_V + 0.35 eV and cannot be observed in DLTS in n-Si.

As one can see in Fig. 4B, The DLTS spectra measured in the same samples in the regions with dislocation density $N_D = 10^5\,cm^{-2}$ (see Fig. 4B) differ significantly from the spectra in dislocation-free regions. In all spectra in Fig. 4B, four broad DLTS lines can be seen that are very similar to typical dislocation-related DLTS lines "A", "B", "C", and "D" observed earlier in many publications [37–40]. In addition, there is one more line at 120 K which in between lines A and B.

Before Fe-in-diffusion (see spectrum (a) in Fig. 4B), the amplitudes of all these lines are quite small, of about (0.2–0.3) x $10^{11}\,cm^{-3}$ for "C" and "D" lines. Iron in-diffusion at 900 °C followed by slow cooling does not result in any significant changes of lines "A", "B", "C", and only the D-line amplitude increased by about 2 times (see spectrum (b) in Fig. 4B). At the same time, quenching after iron in-diffusion results in a significant increase of DLTS lines "C" and "D" (see spectra (c) and (d) in Fig. 4B). Note that the shape and position of "C" and "D" lines are

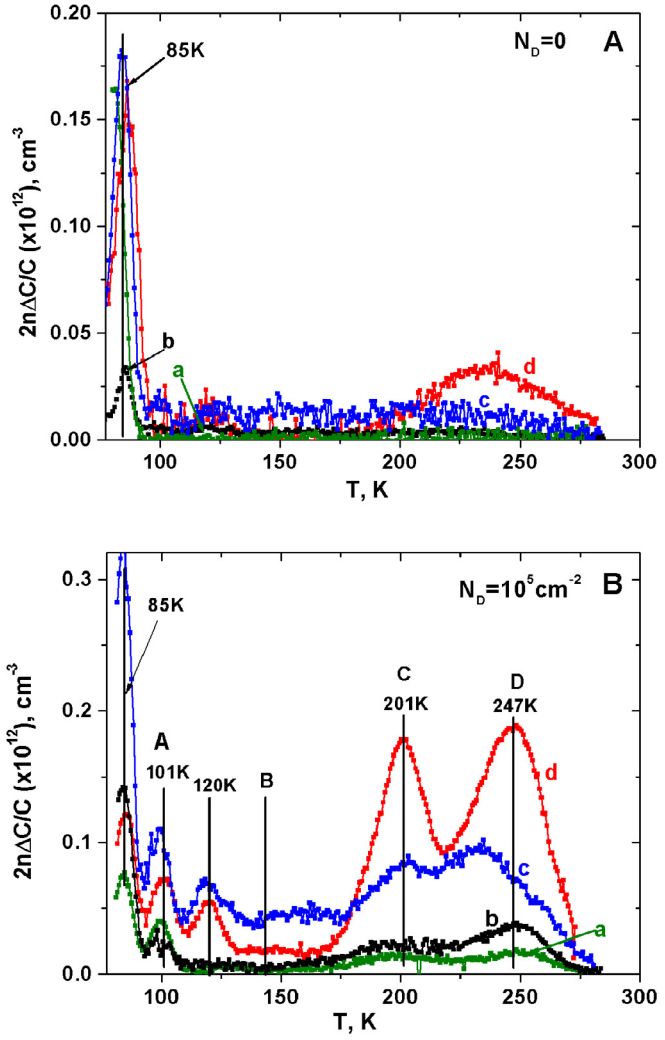

Fig. 4. DLTS spectra in n-Si, measured before and after diffusion of iron at 900 °C: (A) in dislocation-free areas, (B) in the area with $N_D = 10^5\,cm^{-2}$. Spectra "a" - before Fe in-diffusion, "b" - after Fe in-diffusion and slow cooling, "c' - after Fe in-diffusion and quenching to ethylene glycol, "d" - after Fe in-diffusion and quenching to 10% water solution of NaOH. Here n is a phosphorus (dopant) concentration, C is a capacitance of the Schottky diode, ΔC is the amplitude of capacity transient, T is a temperature. DLTS spectra were measured at emission correlation rate $R_{em} = 2.9\ s^{-1}$, refilling pulse duration $t_p = 0.1$ ms, bias voltage $U_b = 5$ V.

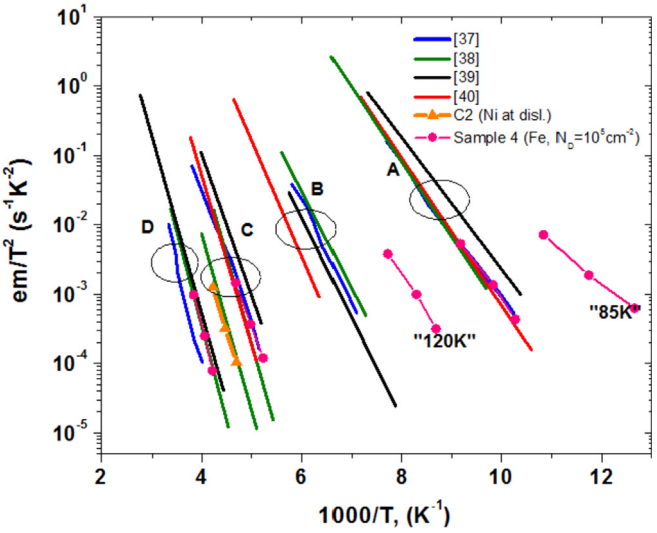

Fig. 5. The solid lines are Arrhenius plots of electron emission rates for dislocation-related DLTS peaks A, B, C, and D was taken from literature. Pink circles show Arrhenius plots of electron emission rates *em* for DLTS peaks observed in n-Si with dislocation density of $N_D = 10^5\,cm^{-2}$ after diffusion of iron and quenching (see spectrum (d) in Fig. 4B).

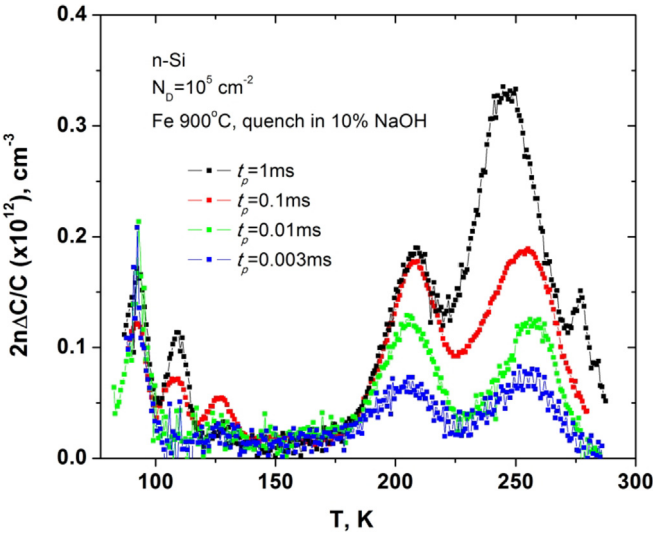

Fig. 6. DLTS spectra in n-Si sample measured after Fe-in-diffusion and quenched in 10% NaOH water solution depending on the refilling pulse duration t_p. Here n is a phosphorus concentration, C is a capacitance of the Schottky diode, ΔC is a capacity transient change, T is a temperature.

slightly different from those in the sample before Fe in-diffusion.

Fig. 5 shows the Arrhenius plot (em/T^2 on $1000/T$) for typical dislocation-related DLTS lines "A", "B", "C", and "D" taken from the literature [37–40] (solid curves). The exact natures of these dislocation-related deep level defects are still unclear. It was shown that the "C" defects correspond to some impurity atoms in at Shockley dislocations [41]. In many cases the C-line in as-deformed samples consists of two different components $C1$ and $C2$ [37]. It means that it may correspond to several types of impurity atoms, or to one and the same impurity in different states. Experiments proved that the high-temperature part of the C-line (the so-called C2-line) is probably associated with nickel atoms at dislocations [11,23,42]. As an example, the orange triangles at Fig. 5 correspond to the C-line measured in n-Si sample with $10^6\,cm^{-2}$ dislocations after Ni in-diffusion [11].

Solid pink circles in Fig. 5 show the positions of DLTS peaks measured in our sample that was quenched in 10% NaOH water solution after Fe-in-diffusion (see spectrum (d) at Fig. 4B). The peak at 101 K is very close to the A-line, while the peak at 201 K is very close to the low-temperature C-line (C1-line), and the peak at 247 K is very close to the D-line.

Note that the amplitudes of the these DLTS peaks depend logarithmically on the refilling pulse duration t_p, i.e. $A \sim \log(t_p)$ (see Fig. 6). Such behavior in n-Si is typical for deep acceptor states localized in some extended defects [39, 43].

We can therefore assume that the peak at 201 K (the "C1-line") and the peak at 247 K (the "D-line") can be associated with iron at dislocations. A good correlation between the amplitudes of DLTS peaks (see Fig. 4B) and the recombination strength of dislocations observed by LBIC (see Fig. 2) supports this assumption.

4. Conclusion

In this paper we investigated the effect of iron atoms on electronic properties of FZ n-Si samples containing dislocations by using DLTS and

LBIC.

According to DLTS measurements, the contamination of samples by about 4×10^{13} cm^{-3} of Fe atoms using in-diffusion at 900 °C in regions without dislocations does not result in an appearance of any significant (more than 3×10^{10} cm-3) concentration of deep level defects in the upper half of Si energy gap, regardless of the cooling rate after Fe-in-diffusion. Their concentration is lower than 3×10^{10} cm^{-3} in all samples (see Fig. 4A).

To explain the decrease of a diffusion length L_D of holes observed by LBIC in dislocation-free regions of all samples after Fe-in-diffusion, we assume that electrically active defects appear there due to reactions of iron with existing vacancy complexes. We suppose that their energy level is in the lower half of the band gap, and therefore they cannot be detected by DLTS in our n-Si samples. This suggestion agrees with the theoretical prediction [24,25] that a {Fe_iV} complex should have the energy level at about E_V + 0.35 eV.

In the regions with 10^5 cm^{-2} dislocations we observed a significant increase of the DLTS peaks at 201 K and 247 K in the samples quenched after iron diffusion. The parameters of these peaks are close to the parameters of the so-called “C1”- and “D” DLTS lines observed earlier by many authors in n-Si with dislocations. In a good correlation with the DLTS data, the LBIC (see Fig. 2) shows a significant decrease of the diffusion length L_D of holes in the vicinity of dislocations in the same samples quenched after Fe-in-diffusion. The amplitude dependency of the broad DLTS peaks C1 at 201 K and D at 247 K on the duration of refilling pulses t_p are typical for deep acceptor levels at extended defects, like dislocations.

Our experimental data can be understood assuming that the iron atoms captured by dislocations result in two types of acceptor states responsible for broad DLTS lines C1 and D. They are also responsible for significant increase of electron-hole recombination at dislocations.

Note that the energy position of the deep level, corresponding to peak “201 K” (C1) calculated from the slope of Arrhenius plot (see Fig. 5.) is E_C - 0.37 eV. This is very close to the deep level $E_{Fe\text{-}dis} = E_V + 0.82$ eV $= E_C - 0.35$ eV predicted theoretically for iron atoms in a dislocation core in Ref. [12]. The nature of peak D at 247 K is less clear. We can assume, for example, that it corresponds to nano-precipitates of iron silicide at dislocations. To confirm these assumptions, additional experiments are required using other research methods, for example TEM.

Acknowledgements

The research was carried out with a partial support of the RFBR grant №18-32-00032 mol-a.

References

[1] S. Woo, M. Bertoni, K. Choi, S. Nama, S. Castellanos, D.M. Powell, T. Buonassisi, H. Choi, An insight into dislocation density reduction in multicrystalline silicon, Sol. Energy Mater. Sol. Cells 155 (2016) 88–100 https://doi.org/10.1016/j.solmat.2016.03.040.

[2] A.A. Istratov, H. Hieslmair, O.F. Vyvenko, E.R. Weber, R. Schindler, Defect recognition and impurity detection techniques in crystalline silicon for solar cells, Sol. Energy Mater. Sol. Cells 72 (2002) 441–451 https://doi.org/10.1016/S0927-0248(01)00192-1.

[3] A.R. Peaker, V.P. Markevich, B. Hamilton, G. Parada, A. Dudas, A. Pap, E. Don, B. Lim, J. Schmidt, L. Yu, Y. Yoon, G. Rozgonyi, Recombination via point defects and their complexes in solar silicon, Phys. Status Solidi 209 (2012) 1884–1893 https://doi.org/10.1002/pssa.201290026.

[4] J. Schmidt, B. Lim, D. Walter, K. Bothe, S. Gatz, T. Dullweber, P.P. Altermatt, Impurity-related limitations of next-generation industrial silicon solar cells, J. Photovoltaics 3 (2013) 114–118 https://doi.org/10.1109/JPHOTOV.2012.2210030.

[5] S. Dubois, O. Palais, P.J. Ribeyron, N. Enjalbert, M. Pasquinelli, S. Martinuzzi, Effect of intentional bulk contamination with iron on multicrystalline silicon solar cell properties, J. Appl. Phys. 102 (2007) 083525 https://doi.org/10.1063/1.2799057.

[6] D. Macdonald, L.J. Geerligs, A. Azzizi, Effect of gettered iron on recombination in diffused regions of crystalline silicon wafers, Appl. Phys. Lett. 85 (2004) 092105 https://doi.org/10.1063/1.2181199.

[7] T. Sadoh, M. Watanabe, H. Nakashima, T. Tsurushima, Deep levels of chromium-hydrogen complexes in silicon, J. Appl. Phys. 75 (1994) 3978 https://doi.org/10.1063/1.356018.

[8] S. Tanaka, H. Kitagawa, Distribution of electrically active nickel atoms in silicon crystals measured by means of deep level transient spectroscopy, Physica B 401–402 (2007) 115–118 https://doi.org/10.1016/j.physb.2007.08.125.

[9] H. Kitagawa, Diffusion and electrical properties of 3d transition-metal impurities in silicon, Solid State Phenom. 71 (2000) 51–72 https://doi.org/10.4028/www.scientific.net/SSP.71.51.

[10] N. Fujita, R. Jones, S. Öberg, P.R. Briddon, A.T. Blumenau, A theoretical study of copper contaminated dislocations in silicon, Solid State Phenom. 131–133 (2008) 259–264 https://doi.org/10.4028/www.scientific.net/SSP.131-133.259.

[11] V. Kveder, M. Khorosheva, M. Seibt, Interplay of Ni and Au atoms with dislocations and vacancy defects generated by moving dislocations in Si, Solid State Phenom. 242 (2016) 147–154 https://doi.org/10.4028/www.scientific.net/SSP.242.147.

[12] B. Ziebarth, M. Mrovec, C. Elsässer, P. Gumbsch, Interstitial iron impurities at cores of dissociated dislocations in silicon, Phys. Rev. B 92 (2015) 195308 https://doi.org/10.1103/PhysRevB.92.195308.

[13] S. Rein, S.W. Glunz, Electronic properties of interstitial iron and iron-boron pairs determined by means of advanced lifetime spectroscopy, J. Appl. Phys. 98 (2005) 113711 https://doi.org/10.1063/1.2106017.

[14] A.A. Istratov, H. Hieslmair, E.R. Weber, Iron and its complexes in silicon, Appl. Phys. A 69 (1999) 13–44 https://doi.org/10.1007/s003390050968.

[15] E. Weber, Transition metals in silicon, Appl. Phys. A 30 (1983) 1–22 https://doi.org/10.1007/BF00617708.

[16] K. Wünstel, P. Wagner, Iron-related deep levels in silicon, Solid State Commun. 40 (1981) 797–799 https://doi.org/10.1016/0038-1098(81)90116-2.

[17] S.D. Brotherton, P. Bradley, A. Gill, Iron and the iron-boron complex in silicon, J. Appl. Phys. 57 (1985) 1941 https://doi.org/10.1063/1.335468.

[18] T. Sadoh, K. Tsukamoto, A. Baba, D. Bai, A. Kenjo, T. Tsurushima, H. Mori, H. Nakashima, Deep level of iron-hydrogen complex in silicon, J. Appl. Phys. 82 (1997) 3828 https://doi.org/10.1063/1.365746.

[19] D. Waiz, J.-P. Joly, G. Kamarinos, On the recombination behaviour of iron in moderately boron-doped p-type silicon, Appl. Phys. A 62 (1996) 345–353 https://doi.org/10.1007/BF01594232.

[20] M. Sanati, N. Gonzalez Szwacki, S.K. Estreicher, Interstitial Fe in Si and its interactions with hydrogen and shallow dopants, Phys. Rev. B 76 (2007) 125204 https://doi.org/10.1103/PhysRevB.76.125204.

[21] M.A. Khorosheva, V.V. Kveder, M. Seibt, On the nature of defects produced by motion of dislocations in silicon, Phys. Status Solidi 212 (2015) 1695–1703 https://doi.org/10.1002/pssa.201532153.

[22] O.V. Feklisova, B. Pichaud, E.B. Yakimov, Annealing effect on the electrical activity of extended defects in plastically deformed p-Si with low dislocation density, Phys. Status Solidi 202 (2005) 896–900 https://doi.org/10.1002/pssa.200460511.

[23] V. Kveder, M. Khorosheva, M. Seibt, Concerning vacancy defects generated by moving dislocations in Si, Mater. Today: Proceedings 5 (2018) 14757–14764 https://doi.org/10.1016/j.matpr.2018.03.065.

[24] M. Sanati, S.K. Estreicher, First-principles study of iron and iron pairs in Si, Physica B 401–402 (2007) 105–108 https://doi.org/10.1016/j.physb.2007.08.123.

[25] S.K. Estreicher, M. Sanati, N. Gonzalez Szwacki, Iron in silicon: interactions with radiation defects, carbon, and oxygen, Phys. Rev. B 77 (2008) 125214 https://doi.org/10.1103/PhysRevB.77.125214.

[26] S. Tanaka, H. Kitagawa, Diffusion and electrical properties of iron-related defects in N-type silicon grown by czochralski- and floating zone method, Jpn, J. Appl. Phys. 37 (1998) 4656–4662 https://doi.org/10.1143/JJAP.37.4656.

[27] A. Onaka-Masada, T. Kadono, N. Mitsugi, K. Kurita, Low-temperature annealing behavior of iron-related deep levels in n-type silicon wafers, Jpn. J. Appl. Phys. 55 (2016) 021301 https://doi.org/10.7567/JJAP.55.021301.

[28] H. Kitagawa, S. Tanaka, B. Ni, In-diffusion and isothermal annealing of iron-related defects in n-type silicon, Jpn. J. Appl. Phys. 32 (1993) L1645 https://doi.org/10.1143/JJAP.32.L1645.

[29] S. Tanaka, H. Kitagawa, Iron-related donor level in N-type silicon, Jpn. J. Appl. Phys. 34 (1995) L721 https://doi.org/10.1143/JJAP.34.L721.

[30] S.D. Brotherton, P. Bradley, A. Gill, Annealing kinetics of the gold-iron complex in silicon, J. Appl. Phys. 57 (1985) 1783 https://doi.org/10.1063/1.334456.

[31] C. Donolato, Theory of beam induced current characterization of grain boundaries in polycrystalline solar cells, J. Appl. Phys. 54 (1983) 1314 https://doi.org/10.1063/1.332205.

[32] W. von Ammon, R. Holzl, J. Virbulis, E. Dornberger, R. Schmolke, D. Gräf, The impact of nitrogen on the defect aggregation in silicon, J. Cryst. Growth 226 (2001) 19 https://doi.org/10.1016/S0022-0248(01)01277-5.

[33] M. Jacob, P. Pichler, H. Ryssel, R. Falster, Determination of vacancy concentrations in the bulk of silicon wafers by platinum diffusion experiments, J. Appl. Phys. 82 (1) (1997) 182 https://doi.org/10.1063/1.365796.

[34] M.A. Khorosheva, V.I. Orlov, N.V. Abrosimov, V.V. Kveder, Determination of the nonequilibrium concentration of vacancies in silicon crystals by measuring the concentration of nickel atoms at lattice sites, J. Exp. Theor. Phys. Lett. 110 (5) (2010), https://doi.org/10.1134/S1063776110050067.

[35] Jack Mullins, Vladimir P. Markevich, Michelle Vaqueiro-Contreras, Nicholas E. Grant, Leif Jensen, Jarosław Jabłonski, John D. Murphy, Matthew P. Halsall, Anthony R. Peaker, Thermally activated defects in float zone silicon: effect of nitrogen on the introduction of deep level states, J. Appl. Phys. 124 (2018) 035701 https://doi.org/10.1063/1.5036718.

[36] P. Pellegrino, P. Leveque, J. Lalita, A. Hallen, C. Jagadish, B.G. Svensson, Annealing kinetics of vacancy-related defects in low-dose MeV self-ion-implanted n-type silicon, Phys. Rev. B 64 (2001) 195211 https://doi.org/10.1103/PhysRevB.64.195211.

[37] D. Cavalcoli, A. Cavallini, E. Gombia, Defect states in plastically deformed n-type silicon, Phys. Rev. B 56 (1997) 10208 https://doi.org/10.1103/PhysRevB.56.10208.
[38] P. Omling, E.R. Weber, L. Montelius, H. Alexander, J. Michel, Electrical properties of dislocations and point defects in plastically deformed silicon, Phys. Rev. B 32 (1985) 6571 https://doi.org/10.1103/PhysRevB.32.6571.
[39] V. Kveder, Yu. Osipyan, W. Schröter, G. Zoth, On the energy spectrum of dislocations in silicon, Phys. Status Solidi 72 (1982) 701 https://doi.org/10.1002/pssa.2210720233.
[40] C. Kisielowski, E.R. Weber, Inhomogeneities in plastically deformed silicon single crystals. II. Deep-level transient spectroscopy investigations of p- and n-doped silicon, Phys. Rev. B 44 (1991) 1600 https://doi.org/10.1103/PhysRevB.44.1600.
[41] V. Kveder, V. Orlov, M. Khorosheva, M. Seibt, Influence of the dislocation travel distance on the DLTS spectra of dislocations in cz-Si, Solid State Phenom. 131–133 (2008) 175–182 https://doi.org/10.4028/www.scientific.net/SSP.131-133.175.
[42] V. Kveder, W. Schröter, M. Seibt, A. Sattler, Electrical activity of dislocations in Si decorated by Ni, Solid State Phenom. 82–84 (2002) 361–366 https://doi.org/10.4028/www.scientific.net/SSP.82-84.361.
[43] W. Schöter, H. Cerva, Interaction of point defects with dislocations in silicon and germanium: electrical and optical effects, Solid State Phenom. 85–86 (2002) 67–144 https://doi.org/10.4028/www.scientific.net/SSP.85-86.67.